

## THE INFLUENCE OF MAGNETIC FIELDS ON ABSORPTION AND EMISSION SPECTROSCOPY

HESHOU ZHANG<sup>1,2</sup>, HUIRONG YAN<sup>1,2</sup> & PHILIPP RICHTER<sup>2,3</sup>

<sup>1</sup>Deutsches Elektronen-Synchrotron DESY, Platanenallee 6, D-15738 Zeuthen, Germany;

<sup>2</sup>Institut für Physik und Astronomie, Universität Potsdam, Haus 28, Karl-Liebknecht-Str. 24/25, D-14476 Potsdam, Germany;

<sup>3</sup>Leibniz-Institut für Astrophysik Potsdam (AIP), An der Sternwarte 16, D-14482 Potsdam, Germany;

### ABSTRACT

Spectroscopic observations play essential roles in astrophysics. They are crucial for determining physical parameters in the universe, providing information about the chemistry of various astronomical environments. However, the analysis of the spectral line intensity in astronomy often does not consider the influence of magnetic fields. In this paper, we explore the influence of magnetic fields on the spectroscopic observations arising from atomic alignment. Synthetic spectra are generated to show the measurable changes of the spectra. The influences of atomic alignment on absorption from Damped Lyman-alpha systems (DLAs), emission from H II Regions, submillimeter fine-structure lines from Star Forming Regions (SFRs) are presented as examples to illustrate the effect in diffuse gas. Furthermore, we illustrate the influence of magnetic fields on physical parameters derived from spectral line ratios, such as the alpha-to-iron ratio ( $[X/Fe]$ ) and ionization rate. Results in our paper show that due to atomic alignment, magnetic fields will affect the spectra of diffuse gas with high signal-to-noise (S/N) ratio with the existence of anisotropic radiation.

*Keywords:* HII regions–ISM: abundances–ISM: lines and bands–magnetic fields–methods: observational–submillimeter: ISM

### 1. INTRODUCTION

Spectroscopy plays a crucial role in studying the universe. Analysing atomic and ionic spectral line intensity<sup>1</sup> is one of the most important part of spectroscopic study. Absorption and emission atomic lines have numerous applications in astronomy. They are direct measurements of column density of lots of elements (e.g., [Fox et al. 2013](#); [Richter et al. 2013](#); [D’Onghia & Fox 2016](#)), and thus help the analysis of chemical evolution and composition of astronomical structures. Physical parameters derived from the spectral line ratio (e.g., ionization rate, temperature) facilitate us to understand the astrophysical environments better (see, e.g., [Draine 1978](#); [Hogerheijde et al. 1995](#); [Salgado et al. 2016](#)). Progress has been made in modelling the physical processes, such as cloud extinction in Photodissociation regions (PDRs) and outflows of Active Galactic Nuclei (AGN), with the help of atomic spectra (e.g., [Kaufman et al. 1999](#); [Coil et al. 2015](#); [Youngblood et al. 2016](#)).

Recent years have seen rapid development in the observation of spectroscopy. In particular, the completion of new telescope and the installation of new camera promise the spectra observed with broader wavelength band, higher resolution and, higher Signal-to-Noise ratio (hereafter, S/N ratio). These developments, while provide us with much more information about the universe, also demand more precise analysis by accounting for more measurable factors that may affect the theoretical interpretations. Astrophysical magnetic field is such a factor that definitely requires more attention. Magnetic fields are ubiquitous in the universe due to the high conductivity of astrophysical fluid. There have been surging interest on the magnetic field and what role it plays in different astrophysical processes owing to the development in theory and polarimetric observations, e.g., from aligned dust grains. It is known that magnetic fields induce line profile broadening of Stokes parameters due to Zeeman effect in the strong field regime. In the weak field regime applicable for the general interstellar medium, however, magnetic fields have usually been neglected in the spectroscopic studies.

In this paper, we will demonstrate that magnetic field has systematic influences on the intensity of atomic and ionic spectral lines observed from diffuse interstellar medium. Absorption and emission spectra of permitted lines and submillimeter fine-structure lines will be studied separately, using typical astrophysical environments as examples. Schematic scenario will be provided for each of the examples. Results of selected representative spectral lines in each scenario will be presented. We shall illustrate that the influence of magnetic field cannot be neglected in spectral line intensity analysis.

<sup>1</sup> Throughout the paper, we address atoms and ions as the term “atoms” for the sake of simplicity.

This paper is organised as follows: The physical effect we use and its applicable regime will be briefly discussed in §2. In §3, synthetic spectra for absorption lines are generated for a schematic study of Damped Lyman-alpha systems (hereby, DLAs) in galaxy to illustrate the influence of the magnetic field on absorption lines. The variation of emission lines induced by magnetic field is demonstrated with the example of extragalactic H II Regions. Results on submillimeter fine-structure lines are presented in Star Forming Regions (SFRs). The influences of magnetic fields on different astrophysical properties derived from spectral line ratios are studied in §4. Discussions and conclusions are provided in §5 and §6.

## 2. INFLUENCE OF MAGNETIC FIELD ON ATOMIC TRANSITIONS

Magnetic field in diffuse medium influences the atomic transitions through the Ground State Alignment (Thereforeforth GSA). Alignment here is in terms of the angular momenta of atoms. GSA is a universal phenomenon in diffuse interstellar medium. Basically it happens wherever the radiation field is anisotropic. The net angular momentum in such radiation field can then be transferred into the atoms. Magnetic field redistributes the angular momenta of atoms in the medium among different sublevels on the ground state, and Therefore modulates the polarizations of scatterings and absorptions from the medium (Yan & Lazarian 2006, 2007, 2008). In addition, it has been also illustrated that GSA influences the line intensities. In this paper, we will adopt GSA effect to study more comprehensively the influence of magnetic fields on the intensity of the absorption and emission spectral lines in diffuse interstellar medium.

GSA has been a well-developed theory. Optical pumping was firstly proposed by Kastler (1950), and then the atomic alignment in the presence of magnetic fields was studied in laboratory (see Hawkins & Dicke 1953; Hawkins 1955; Dehmelt 1957). Toy models of this effect were proposed by Varshalovich (1968, 1971). Then, emission for atoms with an idealized fine structure given a particular geometry of magnetic fields and light beam was discussed in Landolfi & Landi Degl'Innocenti (1986). Calculations in Yan & Lazarian (2006, 2007, 2008) revealed that GSA is a unique tracer for 3D magnetic fields in diffuse interstellar medium (within GSA regime). Zhang et al. (2015) illustrated the existence of GSA in general radiation fields with anisotropy. A detailed study on diagnosing interplanetary magnetic field was conducted in Shangguan & Yan (2013). Spectropolarimetry have been extensively employed to study solar magnetism, which has similarity to GSA but in a totally different regime, i.e. Hanle regime (see, e.g., Landi Degl'Innocenti 1983, 1984, 1998; Stenflo & Keller 1997; Trujillo Bueno & Landi Degl'Innocenti 1997). We will specify the applicable regime for GSA and distinguish it with other effects in the following subsection.

### 2.1. GSA regime

The effective regime of GSA is when  $A$  (emission rate of permitted line)  $\gg \nu_L$  (Larmor precession rate  $\frac{eB}{m_e c}$ )  $\gg \tau_R^{-1}$  (radiative excitation rate  $B_{J_u J_l} I$ )  $\gg \tau_c^{-1}$  (collision rate). This regime, on one hand, means the lifetime of atoms on excited state is much shorter than magnetic precession period. As a result, the influence of magnetic field on excited state is negligible. On the other hand, the magnetic precession frequency is much higher than radiative excitation rates of atoms on the ground state. Thus, the angular momentum of all the atoms on ground state will be altered according to the direction of magnetic field. As long as the magnetic field is within GSA regime, the influence of the magnetic field on the spectra is only sensitive to the magnetic direction. In reality, the upper limit for the strength of magnetic field in the GSA regime is  $1 \text{ Gauss}$ . With magnetic field stronger than  $1 \text{ Gauss}$ , such as the solar magnetism,  $\nu_L$  is comparable to  $A$ . Hanle effect takes place in such case and the influence of magnetic field on upper level cannot be neglected. However, interstellar magnetic fields are normally much weaker. The lower limit for the strength of magnetic field in GSA regime varies with the distance between pumping source and the aligned medium. It is estimated to be smaller than micro Gauss where the diffuse medium is quite close (the distance on the scale of several Au) to the pumping source. Even longer distance from the pumping source to the diffuse medium allows even smaller magnetic fields (down to  $10^{-15} \text{ Gauss}^2$ ) to align the medium. Since the mean magnetic field in the galaxy spiral arm is of the order of  $1 \sim 10 \mu\text{G}$ , spectra observed from the diffuse medium in the galaxy, e.g., DLAs and PDRs, are no doubt in the GSA regime.

### 2.2. Absorption and Emission in GSA Regime

The general theory of GSA has been comprehensively illustrated in the reviews by Yan & Lazarian (2012, 2015). Thus, we briefly highlight the physics for the influence of magnetic field on spectral lines due to GSA. For details about GSA, we refer the readers to the afore mentioned papers.

It is most convenient to calculate atomic alignment in the theoretical frame  $x'y'z'$ -system (Fig.1a), where magnetic direction is  $z'$ -axis. The anisotropic radiation, denoted as  $\Omega_r \equiv (\theta_r, \phi_r)$ , induces the alignment of atomic angular momentum on ground state. Magnetic precession alters the alignment according to the direction of the magnetic field and thus influences the density

<sup>2</sup> Because then the magnetic precession rate is comparable to the radiative pumping rate on the ground level and that is know as lower level Hanle effect (see Yan & Lazarian 2012). It is only a rough estimate here. Specific limits depend not only the distance and type of radiation source, but also the collisions determined by gas density.

tensor of the ground level<sup>3</sup>. We denote the density tensor of the aligned atom on lower level  $J_l$  as  $\rho_Q^K(J_l, \Omega_r)$ <sup>4</sup>. The ratio between the density tensor and the total density of the level is defined as the alignment parameter  $\sigma_Q^K(J_l, \Omega_r) \equiv \rho_Q^K/\rho_0^0$ .

For observational analysis, we adopt the observational frame  $xyz$ -system<sup>5</sup> (see Fig.1b), where the direction of magnetic field is denoted as  $\Omega \equiv (\theta, \phi)$  and  $J_Q^K(i, \Omega)$  is the irreducible radiation tensor of the incoming light. Stokes parameters for absorption lines through the aligned medium with finite optical depth are:

$$\begin{aligned} I &= (I_0 + Q_0)e^{-\tau(1+\frac{\eta_1}{\eta_0})} + (I_0 - Q_0)e^{-\tau(1-\frac{\eta_1}{\eta_0})}, \\ Q &= (I_0 + Q_0)e^{-\tau(1+\frac{\eta_1}{\eta_0})} - (I_0 - Q_0)e^{-\tau(1-\frac{\eta_1}{\eta_0})}, \\ U &= U_0e^{-\tau}, V = V_0e^{-\tau}, \end{aligned} \quad (1)$$

in which  $I_0, Q_0, U_0, V_0$  are the Stokes parameters of the background radiation.  $\eta_i (i = 0 \sim 3)$  are the corresponding absorption coefficients, which are defined as (Landi Degl'Innocenti 1984, see also Yan & Lazarian 2006):

$$\eta_i(\nu, \Omega) = \frac{h\nu_0}{4\pi} Bn(J_l)\Psi(\nu - \nu_0) \sum_{KQ} (-1)^K \omega_{J_l J_u}^K \sigma_Q^K(J_l, \Omega_r) J_Q^K(i, \Omega), \quad (2)$$

where the quantity  $\omega_{J_l J_u}^K \equiv \left\{ \begin{matrix} 1 & 1 & K \\ J_l & J_l & J_u \end{matrix} \right\} / \left\{ \begin{matrix} 1 & 1 & 0 \\ J_l & J_l & J_u \end{matrix} \right\}$ . The quantity B is Einstein coefficient for absorption<sup>6</sup>. The total

atomic population  $n(J_l)$  on the lower level  $J_l$  is defined as  $n\sqrt{[J_l]}\rho_0^0(J_l)$ .  $\Psi(\nu - \nu_0)$  is the line profile. A variation in absorption coefficients  $\eta_i$  will be induced by the change of magnetic direction, and therefore influence the column density of the absorbing species in the optical thin case.

Although the influence of magnetic fields on upper level is negligible in the GSA regime, the alignment on ground state can be transferred to upper states by radiative excitation (see, e.g., Yan & Lazarian 2008):

$$\rho_q^k(J_u, \Omega_r) \sim \sum_{J_l' k'} [J_l'] \left[ \delta_{kk'} p_{k'}(J_u, J_l') B_{lu} I_* J_0^0(0, \Omega_r) + \sum_{Qq'} r_{kk'}(J_u, J_l', Q, q') B_{lu} I_* J_Q^2(0, \Omega_r) \right] \rho_{q'}^{k'}(J_l, \Omega_r). \quad (3)$$

where  $p_k$  and  $r_{kk'}$  are defined in Appendix A. The quantity  $I_*$  is the intensity of the anisotropic radiation. The emission coefficients  $\varepsilon_i (i = 0 \sim 3)$  from the upper level  $J_u$  are (see Yan & Lazarian 2007):

$$\varepsilon_i(\nu, \Omega) = \frac{h\nu_0}{4\pi} A n(J_u) \Psi(\nu - \nu_0) \sum_{KQ} \omega_{J_u J_l}^K \sigma_Q^K(J_u, \Omega_r) J_Q^K(i, \Omega). \quad (4)$$

where the quantity A is Einstein coefficient for emission. Thus, the emissivity  $\varepsilon_0$  is also influenced by the direction of magnetic field due to GSA.

As illustrated earlier in this section, the only property of magnetic field that matters for atomic alignment effect is the magnetic direction. Observational results from different telescope have revealed that the galactic magnetic field bears a uniform component and a random component. The random component has been shown to be predominately parallel to the mean field except for the gas in hot galactic Halo (see, e.g., Brown & Taylor 2001; Crutcher et al. 2003). Therefore, we adopt in general mean magnetic directions<sup>7</sup> to demonstrate schematically the maximum variation of spectral line intensity and do not perform line-of-sight integration in this paper.

Throughout the paper, the case when the magnetic field is parallel to the incidental radiation is set as *case 0*. The influence on spectra is characterized by the ratio between the cases with variations of magnetic field and *case 0*. The variation of magnetic direction is measured in the observational frame (see Fig. 1b). In the following, we will evaluate more quantitatively the influence of magnetic fields on absorption and emission spectral lines due to GSA.

### 3. INFLUENCE ON SPECTRA

#### 3.1. Influence on absorption spectra

<sup>3</sup> Readers may refer to Appendix A for the details.

<sup>4</sup> For example, the irreducible tensor for  $J/F = 1$  is  $\rho_0^2 = [\rho(1,1) - 2\rho(1,0) + \rho(1,-1)]$  (see, e.g., Fano 1957; D'Yakonov & Perel' 1965; Bommiere & Sahal-Brechot 1978).

<sup>5</sup> The transformation between the coordinate systems  $xyz$  and  $x'y'z'$  can be found in Yan & Lazarian (2006).

<sup>6</sup> The data of Einstein coefficients used in the paper are taken from the Atomic Line List (<http://www.pa.uky.edu/~peter/atomic/>) and the NIST Atomic Spectra Database.

<sup>7</sup> The validity of this assumption will be discussed in each example we adopt.

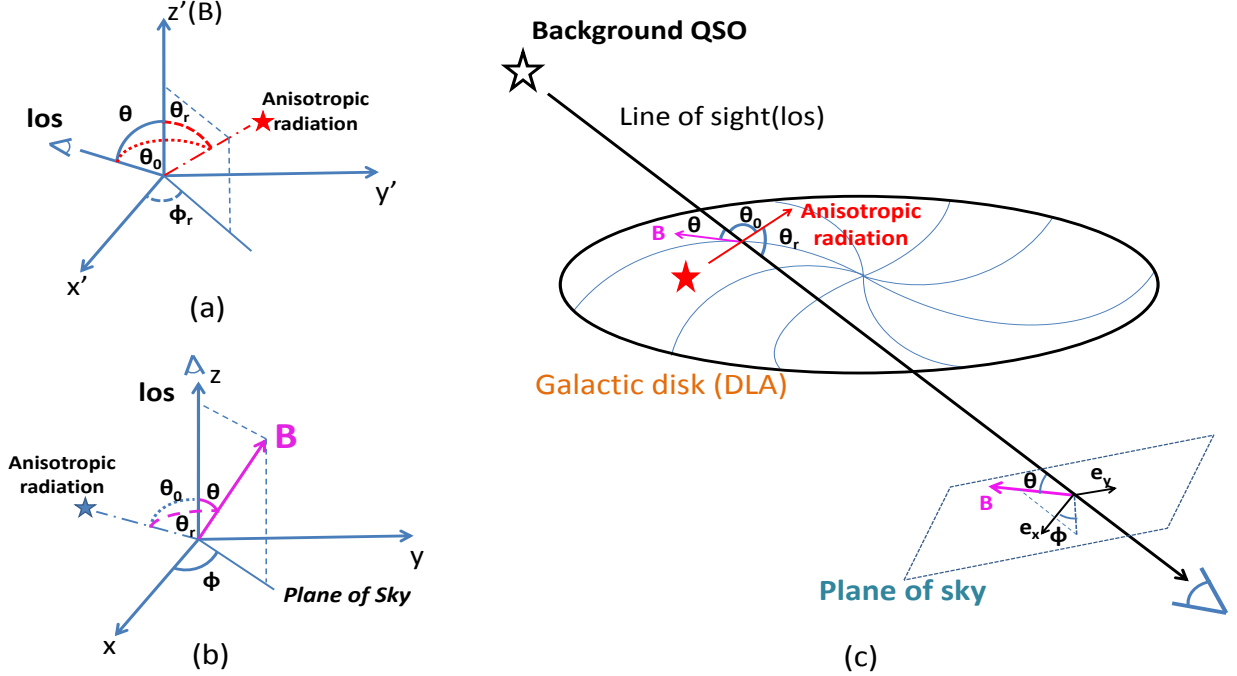


**Figure 1.** (a) Theoretical frame  $x'y'z'$ -coordinate system with the magnetic direction being  $z'$ -axis and line of sight on  $x'z'$ -plane. The direction of anisotropic radiation is  $\Omega_r \equiv (\theta_r, \phi_r)$ . (b) Observational frame  $xyz$ -coordinate system with the line of sight being  $z$ -axis, which is the main coordinate system in the paper since it corresponds directly to the perspective of the observer.  $xy$ -plane is the plane of sky. The direction of magnetic field is  $\Omega \equiv (\theta, \phi)$ . This is the dominant frame for our results. (c) Schematics for the typical environment where absorption lines are observed in the spectra of the QSO behind the region. Alignment of atoms on the ground state in the gas disc is produced by local anisotropic radiation. The magnetic field changes the orientation of the alignment. The absorption lines observed will change in accordance with the change of alignment. The radiation frame uses the direction of radiation as  $z$ -axis, whereas the observational frame uses the line of sight as  $z$ -axis.  $\theta_r, \phi_r$  are the polar and azimuthal angle of the magnetic field in the radiation frame, while  $\theta, \phi$  in the observational frame.  $\theta_0$  is the angle between the anisotropic radiation and the line of sight.

As an example, we show in Fig.1(c) a typical scenario, in which the effect of atomic alignment could lead to measurable effect in observational data. Consider a typical late-type galaxy with an extended neutral gas disk and an interstellar magnetic field. Star-formation is expected to take place in distinct regions in the disk (i.e., in spiral arms). Therefore, the interstellar radiation field is likely to be anisotropic at a given point in the disk. In the spectrum of the background point source (e.g., a Quasi-Stellar Object, hereafter QSO), the gas disk will leave its imprint through many absorption lines from neutral and ionized species, where most of the lines are located in the (rest frame) UV. Such disk absorbers are known to contribute to the population of the so-called DLA absorbers that are frequently observed at low and high redshift in QSO spectra. The DLA absorbers adopted to illustrate the GSA effect are dominated by cold neutral hydrogen (see, e.g., Rao & Turnshek 2000). As illustrated in Crutcher et al. (2003), magnetic fields in such cold H I gas are well ordered in many length scales. Therefore, local magnetic direction can be approximated by the mean field direction. As long as the angle between the ambient magnetic field and the anisotropy of the interstellar radiation field at the place where the sightline pierces the disk is not Van Vleck angle ( $54.7^\circ$  or  $180^\circ - 54.7^\circ$ , Van Vleck 1925; House 1974), the atomic alignment will induce cause small but measurable changes in the central absorption depths of unsaturated absorption lines. Due to the low density in the interstellar medium, the collision rate is much smaller than the Larmor precession rate. Therefore, the magnetic realignment takes place. Below we illustrate how the variation of magnetic field influences intensities of absorptions lines.

The three transitions of singly-ionized sulfur (S II; upper ionization potential 23.3 eV) at  $\lambda\lambda 1250.58, 1253.81, 1259.52$  represent important tracers for neutral and weakly ionized gas in the local interstellar and intergalactic medium and in distant galaxies (e.g., Kisielius et al. 2014; Welsh & Lallement 2012; Richter et al. 2001; Fox et al. 2014a). Sulfur is an  $\alpha$  element, but shows only a weak depletion into dust grains (e.g., Savage & Sembach 1996), so that the interstellar Sulfur abundance is often used as a proxy for the  $\alpha$ -abundance in the gas. The three lines mentioned above span a moderate oscillator strengths (Kisielius et al. 2014; Morton 2003) and the wavelength range of them is within 10 Å. Thus in a UV or optical (if absorption is red-shifted) spectrum, these lines can be observed in the same wavelength region at an identical S/N. In addition, sulfur has a relatively low cosmic abundance (Asplund et al. 2009), so that under typical interstellar conditions (in particular in low-metallicity environments) these

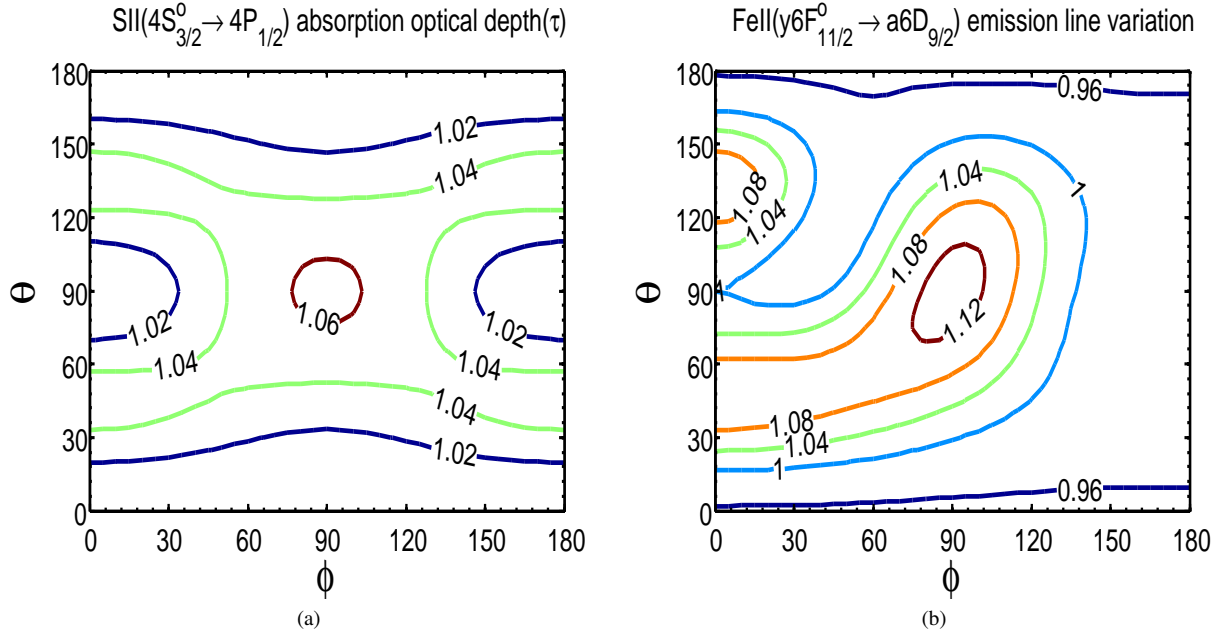


**Figure 2.** Influence of magnetic field on spectral lines of (a) S II  $\lambda 1250.58\text{\AA}$  absorption and (b) Fe II  $\lambda 1143.22\text{\AA}$  emission, respectively, in the case of line of sight vertical to radiation field ( $\theta_0 = 90^\circ$ ).

lines are not saturated. Thus, the S II  $\lambda 1250.58, 1253.81, 1259.52$  represent the ideal transitions to study atomic alignment effects in interstellar environments with magnetic fields. The observed intensity of absorption lines is denoted as  $I_{ob}^{ab}$ , which is proportional to the varied column density  $\tau_0 \pm \Delta\tau$ . The intensity of absorption line in *case 0* is denoted as  $I_0^{ab}$ . The variation ratio is then given by

$$r^{ab}(\lambda, \theta_0, \theta_r, \theta) = I_{ob}^{ab}/I_0^{ab} \propto \left[ \rho_0^0(J_l) \sqrt{2} + \omega_{J_l J_u}^2 \rho_0^2(J_l) (1 - 1.5 \sin^2 \theta) \right], \quad (5)$$

where  $\lambda$  is the wavelength of the line,  $\theta_0, \theta_r, \theta$  are defined in Fig.1. The optical depth variation of S II  $\lambda 1250.58\text{\AA}$  with respect to different magnetic field direction is presented in Fig.2(a) given line of sight perpendicular to radiation direction ( $\theta_0 = 90^\circ$ ), radiation source temperature  $T_{source} = 50000K$ . For the same spectrum with the same radiation field observed from the same line of sight (hereby, the same  $\theta_0$ ), the actual column density deduced from the spectrum can be different only due to the change of magnetic fields. For example, as shown in Fig.2(a), the magnetic field enriches the spectrum by 7% when the direction of the magnetic field is perpendicular to both the line of sight and incident radiation ( $\theta = 90^\circ, \phi = 90^\circ$ ). Thus, *the spectra observed change with the direction of magnetic field.*

Furthermore, we calculate the variation of line intensity of the S II triplet and present in Fig.3 the expected effect of the atomic alignment for the three S II lines in a synthetic absorption spectrum of a DLA for  $\theta_0 = 90^\circ, \theta = 90^\circ, \phi = 90^\circ$ . To show the effect clearly, we zoom in the spectrum to the radial velocity range  $[-10 km \cdot s^{-1}, 10 km \cdot s^{-1}]$ . It is obvious that the alignment enriches  $\lambda 1250.58$  whereas depletes  $\lambda 1253.81$ , and  $\lambda 1259.52$ . Therefore, magnetic field does influence the spectra observed and should be taken into account for the error budget of spectroscopic studies.

Fig.4 illustrates the maximum and minimum column density variations from different absorption lines. Without loss of generality, two cases with (a)  $\theta_0 = 45^\circ$  and (b)  $\theta_0 = 90^\circ$  are presented. The more comprehensive results for maximum and minimum variations of column density for different absorption lines are presented in Table 1<sup>8</sup>, where  $(\Delta N/N_0)_{max}$  means enrichment and  $(\Delta N/N_0)_{min}$  means depletion. As shown in Fig.3, at  $\theta_0 = 90^\circ$ , S II  $\lambda 1250.58$  can be enriched up to 7% whereas S IV  $\lambda 1072.97$  can be depleted up to 27%; S I  $\lambda 1474.57$  can be depleted up to 22% and enriched to the maximum of 2%. Therefore, the influence of magnetic fields changes among different spectral lines, and is sensitive to the direction of the magnetic field.

### 3.2. Magnetic influence on emission spectra

<sup>8</sup> We present not only the absorption from the ground level, but also from some metastable levels that have small energy difference with the ground state and also much longer life time than magnetic precession period. Some of these lines can be detected at the places such as galactic halos (Richter et al. 2013; Fox et al. 2014b) and circumburst medium in GRB (Fynbo et al. 2006). For example, according to Boltzmann distribution, when the medium temperature reaches the scale of a couple of hundred K, the metastable state C II\* ( $J = 3/2$ ) is comparably occupied as the ground state C II ( $J = 1/2$ ) (see Yan & Lazarian 2012).

**Table 1.** COLUMN DENSITY VARIATIONS FOR ABSORPTION LINE

Species	Transition	Wavelength	$(\Delta N/N_0)_{\min}$	$(\Delta N/N_0)_{\max}$
O I	$3P_2 \rightarrow 3D^{\circ}$	1025.76Å	-6.37%	+0%
S I	$3P_2 \rightarrow 3D_1^{\circ}$	1474.57Å	-27.29%	+1.81%
	$3P_2 \rightarrow 3D_2^{\circ}$	1474.38Å	-22.82%	+2.62%
	$3P_2 \rightarrow 3D_3^{\circ}$	1473.99Å	-19.99%	+0.08%
S II	$4S_{\frac{3}{2}}^{\circ} \rightarrow 4P_{\frac{1}{2}}$	1250.58Å	-7.56%	+6.33%
	$4S_{\frac{3}{2}}^{\circ} \rightarrow 4P_{\frac{3}{2}}$	1253.81Å	-4.71%	+7.00%
	$4S_{\frac{3}{2}}^{\circ} \rightarrow 4P_{\frac{5}{2}}$	1259.52Å	-1.61%	+1.22%
Ti II	$a4F_{\frac{3}{2}} \rightarrow z4D_{\frac{3}{2}}^{\circ}$	3072.97Å	-1.64%	+1.30%
	$a4F_{\frac{3}{2}} \rightarrow z4F_{\frac{3}{2}}^{\circ}$	3241.98Å	-1.03%	+1.35%
	$a4F_{\frac{3}{2}} \rightarrow z4F_{\frac{5}{2}}^{\circ}$	3229.19Å	-0.33%	+0.26%
Fe II	$a6D_{\frac{3}{2}} \rightarrow y6F_{\frac{7}{2}}^{\circ}$	1142.36Å	-1.69%	+4.42%
	$a6D_{\frac{3}{2}} \rightarrow y6F_{\frac{9}{2}}^{\circ}$	1143.22Å	-2.86%	+7.94%
	$a6D_{\frac{3}{2}} \rightarrow y6F_{\frac{11}{2}}^{\circ}$	1144.93Å	-0.46%	+3.21%
Absorption from other sublevels of the ground level				
C I*	$3P_1 \rightarrow 3P_0^{\circ}$	1260.93Å	-24.20%	+1.54%
	$3P_1 \rightarrow 3P_1^{\circ}$	1261.00Å	-17.45%	+0.46%
	$3P_1 \rightarrow 3P_2^{\circ}$	1261.12Å	-15.76%	+0%
C II*	$2P_{\frac{3}{2}}^{\circ} \rightarrow 2S_{\frac{1}{2}}$	1037.02Å	-9.02%	+3.68%
	$2P_{\frac{3}{2}}^{\circ} \rightarrow 2D_{\frac{3}{2}}$	1335.66Å	-10.34%	+1.29%
	$2P_{\frac{3}{2}}^{\circ} \rightarrow 2D_{\frac{5}{2}}$	1335.71Å	-5.39%	+0.10%
O I*	$3P_1 \rightarrow 3D^{\circ}$	1027.43Å	-9.57%	+0%
Si II*	$2P_{\frac{3}{2}}^{\circ} \rightarrow 2D_{\frac{3}{2}}$	1264.74Å	-5.59%	+5.32%
	$2P_{\frac{3}{2}}^{\circ} \rightarrow 2D_{\frac{5}{2}}$	1265.00Å	-3.00%	+0.27%
S I*	$3P_1 \rightarrow 3P_0^{\circ}$	1303.11Å	-21.05%	+1.72%
	$3P_1 \rightarrow 3P_1^{\circ}$	1302.86Å	-14.43%	+0.50%
	$3P_1 \rightarrow 3P_2^{\circ}$	1302.34Å	-12.74%	+0%
S III*	$3P_1 \rightarrow 3P_0^{\circ}$	1015.50Å	-24.67%	+1.53%
	$3P_1 \rightarrow 3P_1^{\circ}$	1015.57Å	-17.88%	+0.46%
	$3P_1 \rightarrow 3P_2^{\circ}$	1015.78Å	-16.19%	+0%
S IV*	$2P_{\frac{3}{2}}^{\circ} \rightarrow 2D_{\frac{3}{2}}$	1072.97Å	-1.20%	+2.20%
	$2P_{\frac{3}{2}}^{\circ} \rightarrow 2D_{\frac{5}{2}}$	1073.52Å	-0.20%	+0.56%
C I**	$3P_2 \rightarrow 3D_1^{\circ}$	1193.65Å	-24.65%	+1.06%
	$3P_2 \rightarrow 3D_2^{\circ}$	1193.39Å	-20.93%	+1.51%
	$3P_2 \rightarrow 3D_3^{\circ}$	1193.24Å	-18.74%	+0%
S III**	$3P_2 \rightarrow 3D_1^{\circ}$	1202.12Å	-24.20%	+0.95%
	$3P_2 \rightarrow 3D_2^{\circ}$	1201.73Å	-20.62%	+1.37%
	$3P_2 \rightarrow 3D_3^{\circ}$	1200.97Å	-18.53%	+0%

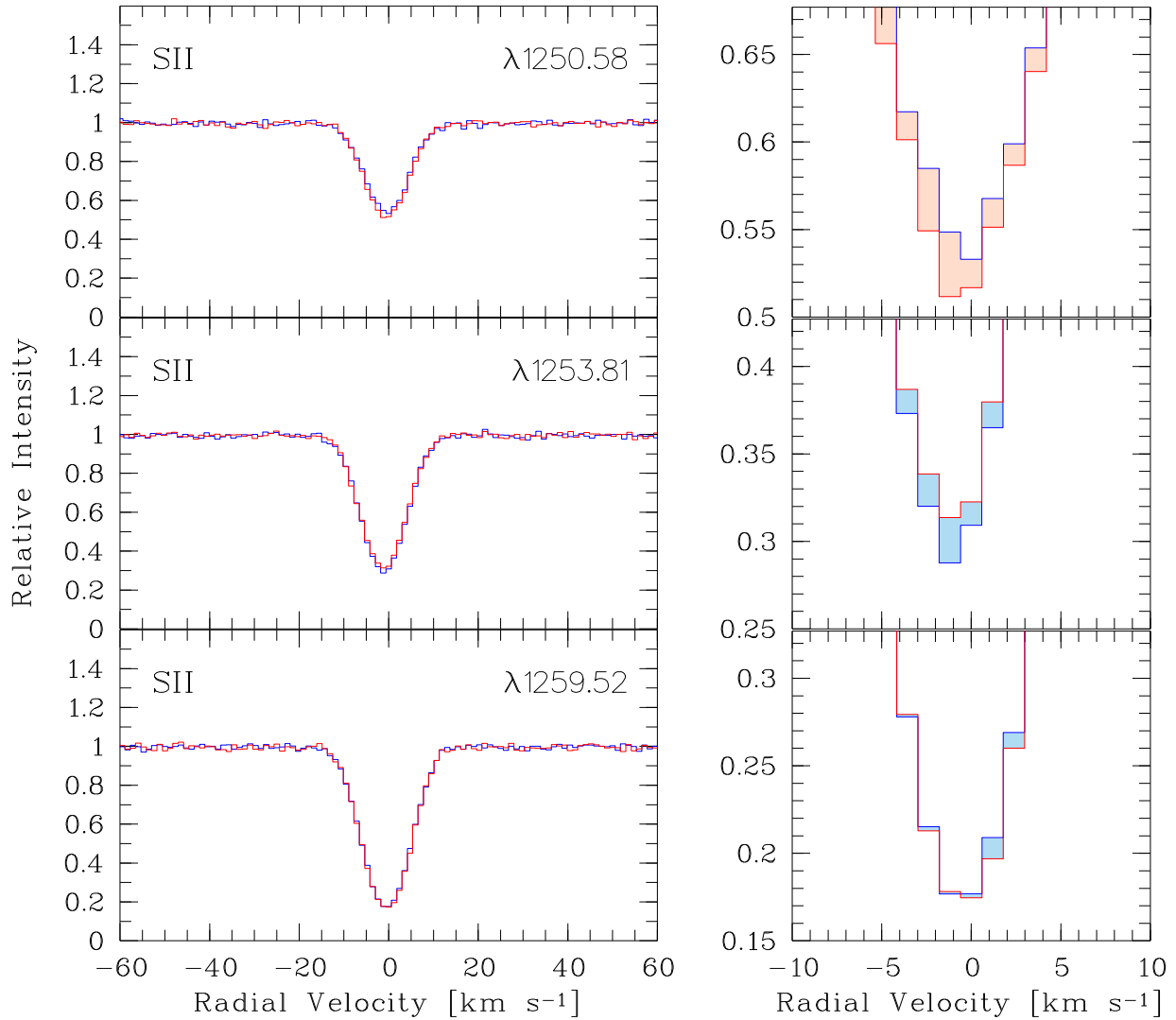


**Figure 3.** Synthetic spectrum (in velocity scale) of a single-component S II  $\lambda\lambda 1250.58, 1253.81, 1259.52$  absorption system with a S II column density of  $N(\text{S II}) = 4 \times 10^{14} \text{ cm}^{-2}$ , a Doppler parameter of  $b = 5 \text{ km s}^{-1}$ , a spectral resolution of  $R = 45,000$ , and a S/N of 100 per resolution element. Such a S II column density would be expected for a DLA with  $\log N(\text{H I}) = 20.48$  and a sulfur abundance of 0.1 solar assuming solar reference abundances of [Asplund et al. \(2009\)](#). The synthetic spectra were generated using the FITLYMAN routine ([Fontana & Ballester 1995](#)) implemented in the ESO-MIDAS software package. Atomic data were taken from [Morton \(2003\)](#). The blue solid line shows the original spectrum without the atomic alignment, the red solid lines shows the spectrum including the alignment effect, assuming  $\theta_0 = \theta = 90^\circ$ ,  $\phi = 0$ . The red/blue-shaded areas indicate the excess/deficiency of absorption due to the alignment effect.

Emission spectra are very important in astrophysical studies. UV emission lines are used to model stellar wind ([Leitherer et al. 2016](#)). Optical recombination emission lines can help the analysis of chemical abundance in H II regions and Planetary Nebulae (PNe) (e.g., [García-Rojas et al. 2016](#); [Peimbert & Peimbert 2006](#)), and they have the advantages that they are not severely affected by the uncertainty of reddening correction associated with collision excited lines and they can be used directly to analyse the chemistry in ionized gas phase (e.g., [Esteban et al. 2014](#)). Combined with absorption spectra, emission spectra can provide even more information, e.g., gas condition in DLAs (e.g., [Meiring et al. 2011](#); [Kisielius et al. 2014](#)). In this section we will illustrate the influence of magnetic field on emission spectra from diffuse gas due to GSA effect.

As an example, we show in [Fig. 5](#) a typical scenario, where GSA affects the observational emission data. Presented is a typical diffuse emission nebulae (e.g., diffuse PDRs or H II regions) denoted in dashed arch with embedded magnetic field. The size span of H II regions is of the order of 1 pc or smaller. The coherence length of interstellar magnetic field is much larger ( $100 \text{ pc}$  from the diagnosis of the magnetohydrodynamic turbulence in ISM, see [Armstrong et al. 1995](#); [Chepurnov et al. 2008](#)). Therefore the mean field approach is also justified. Stars in the H II region ionise and illuminate the surrounding medium, from which the

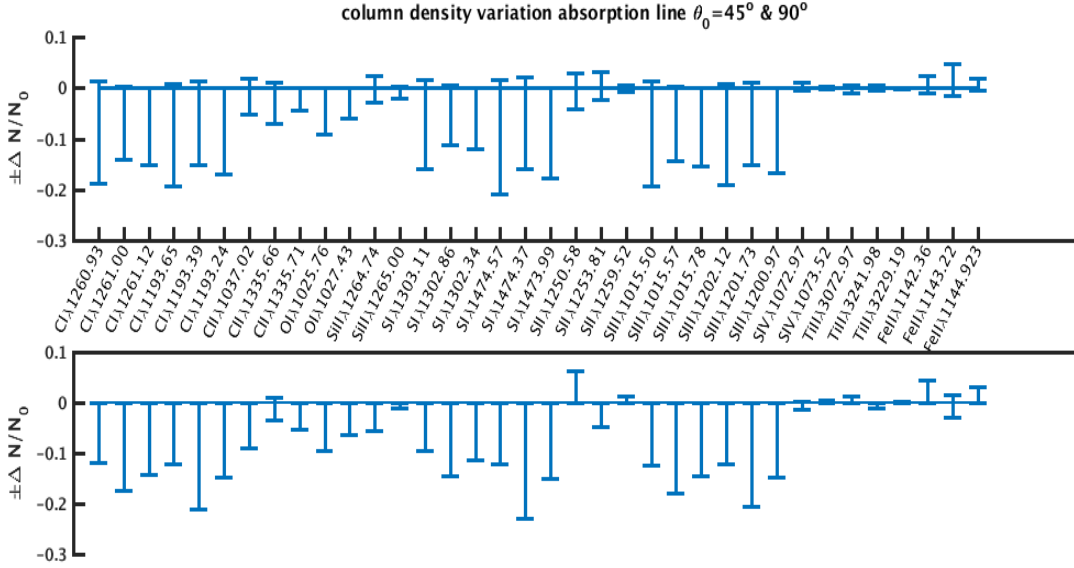


**Figure 4.** Measurements on the variation of column density from absorption lines. Maximum and minimum column density variations for *upper*:  $\theta_0 = 45^\circ$  and *lower*:  $\theta_0 = 90^\circ$  are presented, respectively. Value above 0 means enrichment while below means depletion. Atoms are listed in the order of element number.

emission lines can be observed. Radiation field here<sup>9</sup> is expected to have a certain degree of anisotropy. As illustrated in §2.1, the influence of magnetic field on excited states is negligible in GSA regime. Nevertheless, with the influence of magnetic fields and anisotropic radiation field, the ground state of the atoms in diffuse gas will be aligned and the alignment will be transferred to upper states due to radiative excitations. This scattering process with imprinted GSA will cause measurable changes in the emission spectra observed. Small density of the diffuse medium in H II region promises a much smaller collision rate than Larmor precession rate, which makes GSA happen.

Different from the case of absorption lines, GSA for emission lines is a scattering process. Given  $i = 0$  in Eq. 4, the intensity of the emission lines can be expressed by:

$$I_{em}(\nu, \Omega) = \frac{h\nu_0}{4\pi} A_n(J_u, \theta_r) \Psi(\nu - \nu_0) \sum_{KQ} \omega_{J_u J_l}^K \sigma_Q^K(J_u, \Omega_r) g_Q^K(0, \Omega). \quad (6)$$

The observed intensity of emission line is denoted as  $I_{ob}^{em}$ . The intensity of emission line in *case 0* is denoted as  $I_0^{em}$ . The ratio between observed line intensity and *case 0* for emission lines is:

$$r^{em}(\lambda, \theta_0, \theta_r, \theta) = I_{ob}^{em} / I_0^{em} \propto \left[ \rho_0^0(J_u) \sqrt{2} + \sum_Q \omega_{J_u J_l}^2 \rho_Q^2(J_u, \Omega_r) g_Q^K(0, \Omega) \right], \quad (7)$$

where  $\lambda$  is the wavelength of the line,  $\theta_0, \theta_r, \theta$  are defined in Fig.1,  $Q = 0, \pm 1, \pm 2$ ,  $\rho_Q^2(J_u)$  is defined in Eq. (3).

We adopt Fe II emission lines as an example. Fe II emission spectra in UV and optical band are an important tool for modelling Planetary Nebulae (PNe) (Dinerstein et al. 2006) and cloud near AGNs (Wills et al. 1985). The ground state of Fe II has 5 sublevels  $a6D_{\frac{1}{2}, \frac{3}{2}, \frac{5}{2}, \frac{7}{2}, \frac{9}{2}}$ , in which the ground level is  $a6D_{\frac{9}{2}}$ . There are many upper states for Fe II. The selected emission line we study in this paper are from the excited state  $y6F_{\frac{11}{2}}^o$  to the ground state  $a6D_{\frac{9}{2}}$ . We emphasize the influence of magnetic fields on line intensity also exists in other emission transitions. The influence of magnetic field on Fe II emission line with the wavelength  $\lambda 1144.93$  when  $\theta_0 = 90^\circ$  are presented in Fig.2(b). For the same spectrum with the same  $\theta_0$ , the line intensity observed can be different only due to the change of magnetic direction. As demonstrated in Fig.2(b), the magnetic field enriches more than 10% of the spectrum when the magnetic field is perpendicular to both the line of sight and incident radiation ( $\theta = 90^\circ, \phi = 90^\circ$ ). Therefore, it is necessary to account for the variations in the spectrum observed induced by GSA.

Fig.7(a) provides an overview on the maximum and minimum intensity variations of different emission lines with the radiation source again in the two directions: (a)  $\theta_0 = 45^\circ$  and (b)  $\theta_0 = 90^\circ$ . The more comprehensive results for maximum and minimum variations of intensity for different spectral lines are presented in Table 2, where  $(\Delta I/I_0)_{\max}$  means enrichment and  $(\Delta I/I_0)_{\min}$

<sup>9</sup> As illustrated in Zhang et al. (2015), alignment also exists in extended radiation source (e.g., cluster of stars). For simplicity, the radiation source considered here has been treated as a point source.

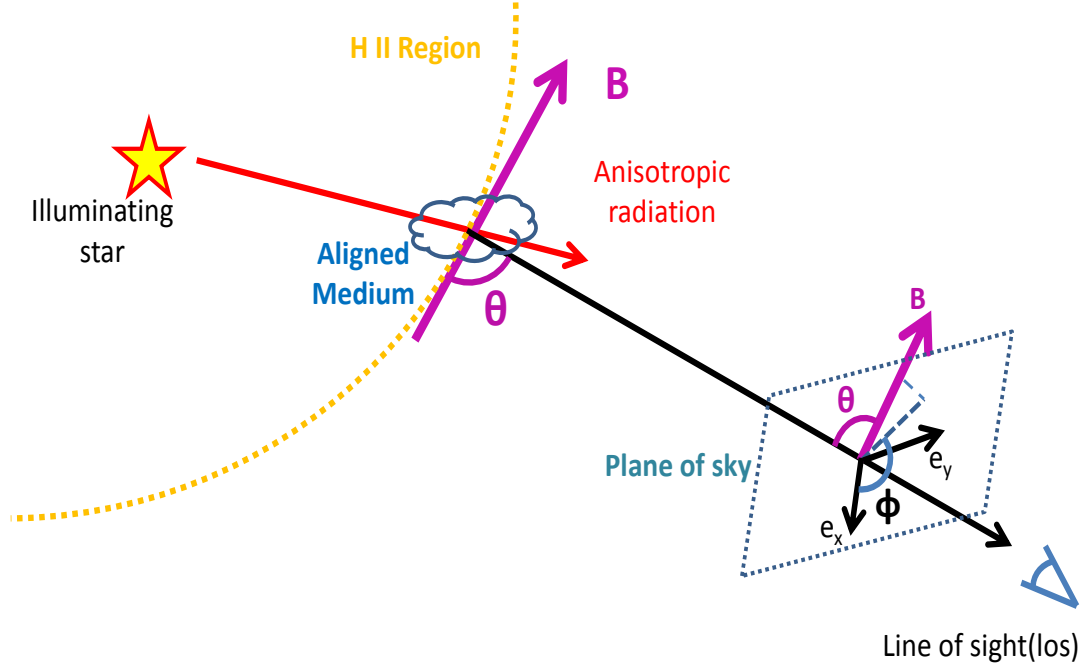


**Figure 5.** Scenario for atomic alignment for emission lines in extragalactic H II region. H II regions (denoted in dashed arch) is a typical environment where emission spectra are affected by GSA. Alignment on ground state is produced by anisotropic radiation field and alters according to the direction of magnetic field. Stars illuminate surrounding medium which gives emission lines. When the illumination happens to the aligned medium, the density of excited state is also affected by the alignment on the ground state (See Eq. (3)). As a result, the emission from illuminated medium can also be influenced by GSA effect. Simplified plots for the geometry in the observational frame can be found in Fig.1(b).

means depletion. For  $\theta_0 = 90^\circ$ , S II  $\lambda 1259.52$  can be depleted to the maximum of more than 6% and enriched up to 22%; S I  $\lambda 1473.99$  can be depleted to the maximum of more than 25% whereas the line S II  $\lambda 1253.81$  can be enriched up to 38% , as demonstrated in Fig.7(a). Thus, it is clear that magnetic fields have influence on emission spectra. The influence varies among different spectral lines and is sensitive to the direction of the magnetic field.

**Table 2.** LINE INTENSITY VARIATIONS FOR EMISSION LINE

Species	Transition	Wavelength	$(\Delta I/I_0)_{\min}$	$(\Delta I/I_0)_{\max}$
C I	$3D_1^{\circ} \rightarrow 3P_0$	1193.03Å	-20.85%	+21.00%
C II	$2S_{3/2}^{\circ} \rightarrow 2P_{1/2}^{\circ}$	1334.53Å	-29.17%	+28.90%
O I	$3D^{\circ} \rightarrow 3P_2$	1025.76Å	-14.30%	+10.44%
Si II	$2P_{3/2}^{\circ} \rightarrow 2P_{1/2}^{\circ}$	1190.42Å	-27.20%	+31.49%
S I	$3D_1^{\circ} \rightarrow 3P_2$	1474.57Å	-6.32%	+0.50%
	$3D_2^{\circ} \rightarrow 3P_2$	1474.38Å	-19.62%	+7.49%
	$3D_3^{\circ} \rightarrow 3P_2$	1473.99Å	-38.67%	+3.89%
S II	$4P_{3/2}^{\circ} \rightarrow 4S_{3/2}^{\circ}$	1253.81Å	-20.51%	+38.79%
	$4P_{1/2}^{\circ} \rightarrow 4S_{3/2}^{\circ}$	1259.52Å	-23.04%	+21.27%
S III	$3P_1^{\circ} \rightarrow 3P_0$	1012.50Å	-32.02%	+6.01%
S IV	$2D_{3/2}^{\circ} \rightarrow 2P_{1/2}^{\circ}$	1062.66Å	-35.44%	+44.09%
Fe II	$y6F_{7/2}^{\circ} \rightarrow a6D_{9/2}$	1142.36Å	-2.90%	+12.10%
	$y6F_{9/2}^{\circ} \rightarrow a6D_{9/2}$	1143.22Å	-9.37%	+22.44%
	$y6F_{11/2}^{\circ} \rightarrow a6D_{9/2}$	1144.93Å	-14.38%	+13.64%

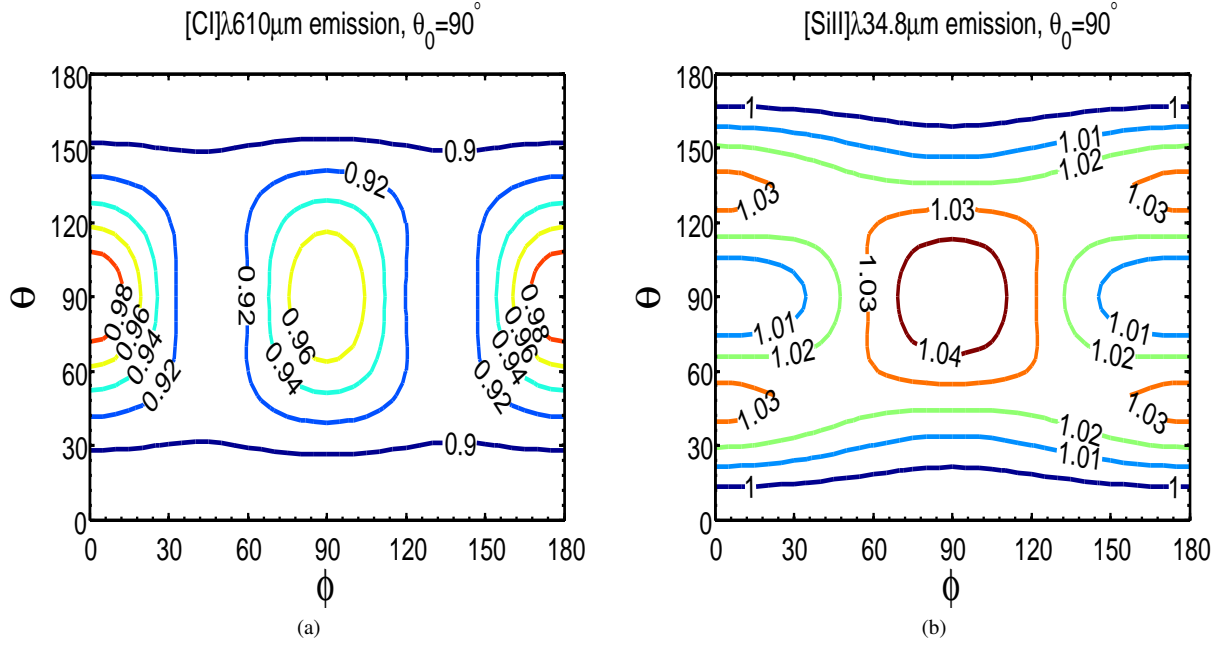


**Figure 6.** The variation of line intensity for submillimeter lines with respect to the direction of the magnetic field due to GSA for (a) C I  $\lambda 610 \mu\text{m}$  and (b) Si II  $\lambda 34.8 \mu\text{m}$  when  $\theta_0 = 90^\circ$ .

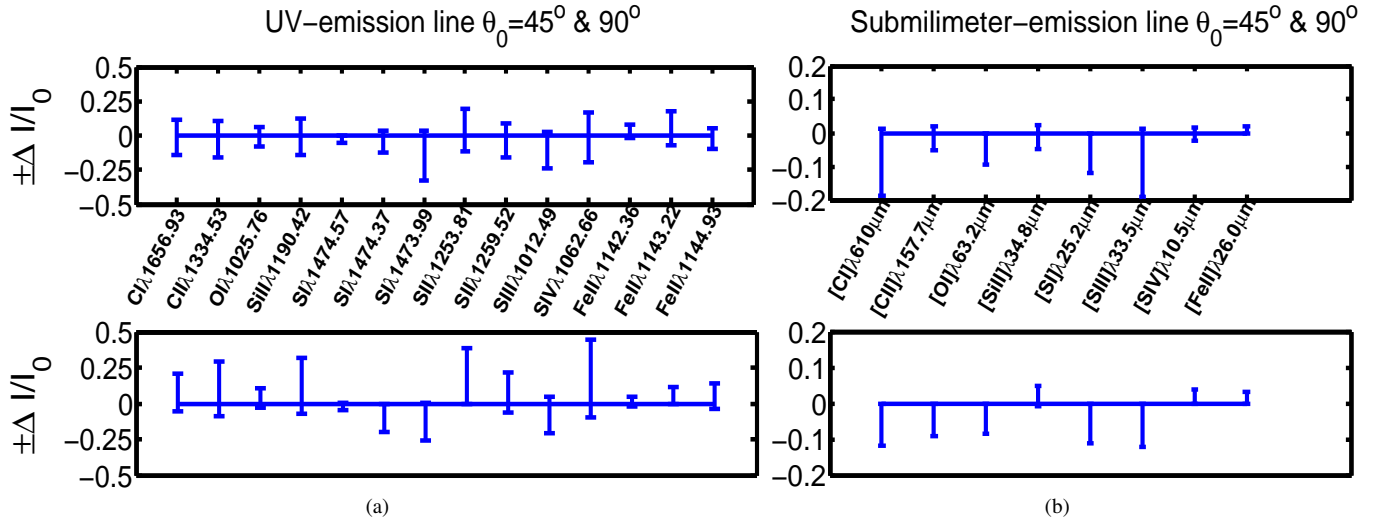


**Figure 7.** Measurements on the variation of column density from (a) emission and (b) submillimeter fine-structure lines. Maximum and minimum column density variations for *upper*:  $\theta_0 = 45^\circ$  and *lower*:  $\theta_0 = 90^\circ$  are presented, respectively. Value above 0 means enrichment while below means depletion. Atoms are listed in the order of element number. Only transitions to the ground level are considered.

### 3.3. Magnetic influence on submillimeter fine-structure lines

Submillimeter fine-structure spectra, which arise from magnetic dipole transitions, have a broad applicability in astrophysics. Submillimeter lines can be used to determine chemical properties of distant star-forming galaxies and derive electron and ionization temperature of galaxy (Kobulnicky et al. 1999). They can be applied to predicting star burst size (Díaz-Santos et al. 2013). They also help the modelling of flaring Herbig Ae/Be disks (Maaskant et al. 2013).

However, previous studies do not consider atomic alignment, which in two aspects influences the results. First, in real circumstances, the assumption that radiation field is isotropic can be problematic. For example, in protoplanetary disks, dominant radiation source could be localized (see Appendix A in Kama et al. 2016 for details). Moreover, the magnetic realignment has to be taken into consideration. Thus, as discussed in §2, emission and absorption coefficients for Stokes parameters will be modified due to atomic alignment.

For submillimeter fine-structure lines, the absorption process is exactly the same as the case in §3.1. Thus, we only study emission lines in this section. The emission process, nevertheless, is different from the emission we discussed in §3.2. The upper level of submillimeter emission line is meta-stable. The life-time of atoms on the meta-level can be considered much longer than the emission rate  $A_m$  because the emission rate of magnetic dipole transitions within the lower levels is much smaller than the permitted emission rate (e.g.,  $A_m([\text{C II}])/A(\text{C II } \lambda 1335.71 \text{ \AA}) \sim 10^{-14}$ ). As a result, the excited state here is also aligned. For example, the influence of atomic alignment on C I  $\lambda 610 \mu\text{m}$  and Si II  $\lambda 34.8 \mu\text{m}$  lines are presented in Fig.6. The ground state of C I has 3 sublevels  $3P_{0;1;2}$ , in which the ground level is  $3P_0$ . C I  $\lambda 610 \mu\text{m}$  line represents the emission within lower sublevels from  $3P_1$  to  $3P_0$ . The ground state of Si II has two sublevels  $2P_{\frac{1}{2};\frac{3}{2}}^o$ , in which the ground sublevel is  $2P_{\frac{1}{2}}^o$ . Si II  $\lambda 34.8 \mu\text{m}$  line represents the emission from  $2P_{\frac{3}{2}}^o$  to  $2P_{\frac{1}{2}}^o$ . As demonstrated in Fig.6(a), atomic alignment can induce different modification to spectral lines with respect to the magnetic direction. In addition, for the same geometry, atomic alignment can deplete C I  $\lambda 610 \mu\text{m}$  line by a factor of more than 8% and enrich Si II  $\lambda 34.8 \mu\text{m}$  line by a factor of around 3% when  $\theta = 60^\circ$ . Thus, the influence of magnetic field on submillimeter fine-structure lines also depends the magnetic direction and varies with the wavelength.

Fig.7(b) provides an overview on the maximum and minimum column density variations with  $\theta_0 = 45^\circ$  and  $\theta_0 = 90^\circ$  for different submillimeter fine-structure lines, respectively. Table 3 presents the influence of atomic alignment on different submillimeter lines, where  $(\Delta I/I_0)_{\text{max}}$  means enrichment and  $(\Delta I/I_0)_{\text{min}}$  means depletion. It is clear that magnetic fields have different influences on different spectral lines. For example, for  $\theta_0 = 45^\circ$ , S III  $\lambda 33.5 \mu\text{m}$  can be enriched to the maximum of more than 2% and depleted up to almost 20% only depending only on the direction of the magnetic field; Si II  $\lambda 34.8 \mu\text{m}$  can be enriched to the maximum of around 3% whereas C I  $\lambda 610 \mu\text{m}$  can be depleted up to almost 20%, as illustrated in Fig.7(b).

**Table 3.** LINE INTENSITY VARIATIONS FOR SUBMILLIMETER LINE

Species	Transition	Wavelength	$(\Delta I/I_0)_{\text{min}}$	$(\Delta I/I_0)_{\text{max}}$
[C I]	$3P_1 \rightarrow 3P_0$	$610 \mu\text{m}$	-24.2%	+1.54%
[C II]	$2P_{3/2}^o \rightarrow 2P_{1/2}^o$	$157.7 \mu\text{m}$	-9.02%	+3.68%
[O I]	$3P_1 \rightarrow 3P_2$	$63.2 \mu\text{m}$	-10.77%	+0%
[Si II]	$2P_{3/2}^o \rightarrow 2P_{1/2}^o$	$34.8 \mu\text{m}$	-8.76%	+4.90%
[S I]	$3P_1 \rightarrow 3P_2$	$25.2 \mu\text{m}$	-12.73%	+0%
[S III]	$3P_1^o \rightarrow 3P_0$	$33.5 \mu\text{m}$	-24.67%	+1.53%
[S IV]	$2P_{3/2}^o \rightarrow 2P_{1/2}^o$	$10.5 \mu\text{m}$	-2.04%	+2.00%
[Fe II]	$a6D_{7/2} \rightarrow a6D_{9/2}$	$26.0 \mu\text{m}$	-0.39%	+3.11%

#### 4. INFLUENCE ON PHYSICAL PARAMETERS DERIVED FROM LINE RATIO

Many important physical parameters in astronomy are derived from spectral line ratio. For example, the ratio of different transitions of C II ( $\lambda 1036.34$  and  $\lambda 1334.53$ ) is used to estimate the electron density in different astrophysical environments (see Lehner et al. 2004; Zech et al. 2008; Richter et al. 2013 for details). According to Eq. (5), the ratio of line intensity between two different absorption lines is given by

$$\begin{aligned} \mathcal{R}_{\lambda_1, \lambda_2}^{ab}(\theta_0, \theta_r, \theta) &= r^{ab}(\lambda_1, \theta_0, \theta_r, \theta) / r^{ab}(\lambda_2, \theta_0, \theta_r, \theta), \\ &\propto \frac{\rho_0^0(J'_l) \sqrt{2} + \omega_{J'_l J'_u}^2 \rho_0^2(J'_l, \Omega_r) (1 - 1.5 \sin^2 \theta')}{\rho_0^0(J_l) \sqrt{2} + \omega_{J_l J_u}^2 \rho_0^2(J_l, \Omega_r) (1 - 1.5 \sin^2 \theta)}. \end{aligned} \quad (8)$$

And the ratio of intensities of two emission lines can be obtained from Eq. (7):

$$\begin{aligned} \mathcal{R}_{\lambda_1, \lambda_2}^{em}(\theta_0, \theta_r, \theta) &= r^{em}(\lambda_1, \theta_0, \theta_r, \theta) / r^{em}(\lambda_2, \theta_0, \theta_r, \theta), \\ &\propto \frac{\rho_0^0(J'_u) \sqrt{2} + \sum_Q \omega_{J'_u J'_l}^2 \rho_Q^2(J'_u) \mathcal{J}_Q^K(0, \Omega)}{\rho_0^0(J_u) \sqrt{2} + \sum_Q \omega_{J_u J_l}^2 \rho_Q^2(J_u) \mathcal{J}_Q^K(0, \Omega)}. \end{aligned} \quad (9)$$

As illustrated in §3, the influence of GSA on different spectral lines is different even with the same direction of magnetic field. Therefore, the influence on spectral line ratio can be expected to be more significant, e.g., with one line depleted and the other enriched. A few examples will be presented in the following subsections.

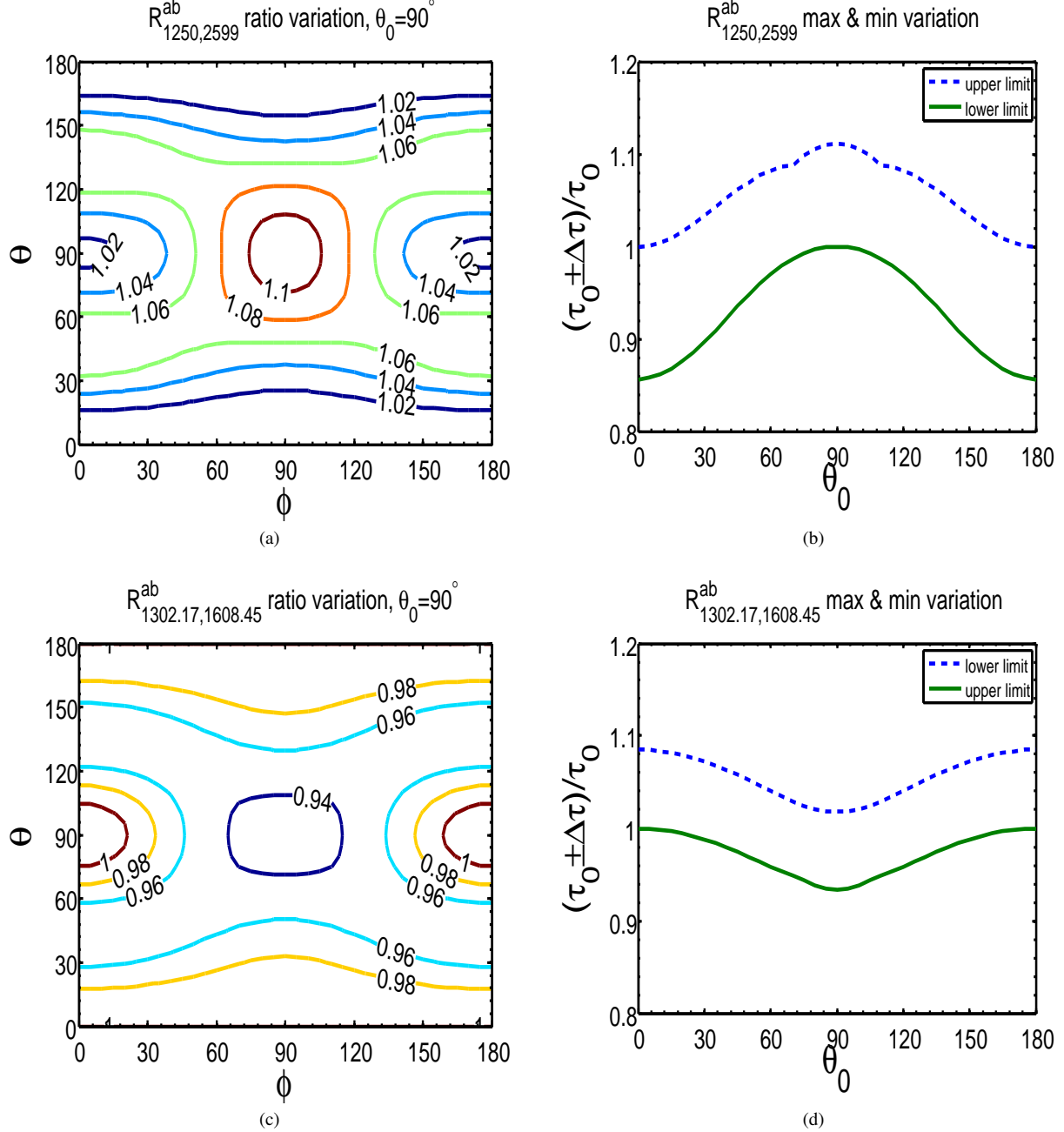


**Figure 8.**  $[\alpha/\text{Fe}]$  ratio using S II  $\lambda 1250/\text{Fe II } \lambda 2599$  and O I  $\lambda 1302.17/\text{Fe II } \lambda 1608.45$  absorption line ratios. The variation is compared with case 0. (a),(c) The variation of line ratio  $R_{1250,2599}^{ab}$  and  $R_{1302.17,1608.45}^{ab}$  with respect to the direction of the magnetic field when  $\theta_0 = 90^\circ$ ; (b),(d) The maximum and minimum variation of line ratio  $R_{1250,2599}^{ab}$  and  $R_{1302.17,1608.45}^{ab}$  for different  $\theta_0$ .

#### 4.1. Influence on nucleosynthetic studies in DLAs

The alpha-to-iron ratio is widely used in spectral analysis. This line ratio comparison reflects the nucleosynthetic processes in star forming region (e.g., Prochaska et al. 2001; Prochaska & Wolfe 2002). The  $\alpha$  elements include O, Si, S, Ti, etc. Iron refers to Fe peak elements such as Cr, Mn, Co, Fe, etc.  $\alpha$  elements in the medium of the galaxy with low metallicity ( $[\text{Fe}/\text{H}] \lesssim -1.0$ ) are produced exclusively by Type-II supernovae (SNe II), but the  $[\alpha/\text{Fe}]$  ratio suffers a drop when the delayed contribution of Fe from Type-Ia supernovae (SNe Ia) is effective (McWilliam 1997; Cooke et al. 2011). The alpha-to-iron ratio  $[\text{X}/\text{Fe}]$  (X represents the chemical elements for  $\alpha$  elements) is defined by the ratio of abundance observed from the medium in comparison with that from the sun:

$$[\text{X}/\text{Fe}] \equiv \log[\text{N}(\text{X})/\text{N}(\text{Fe})] - \log[\text{N}(\text{X})/\text{N}(\text{Fe})]_{\odot} \quad (10)$$

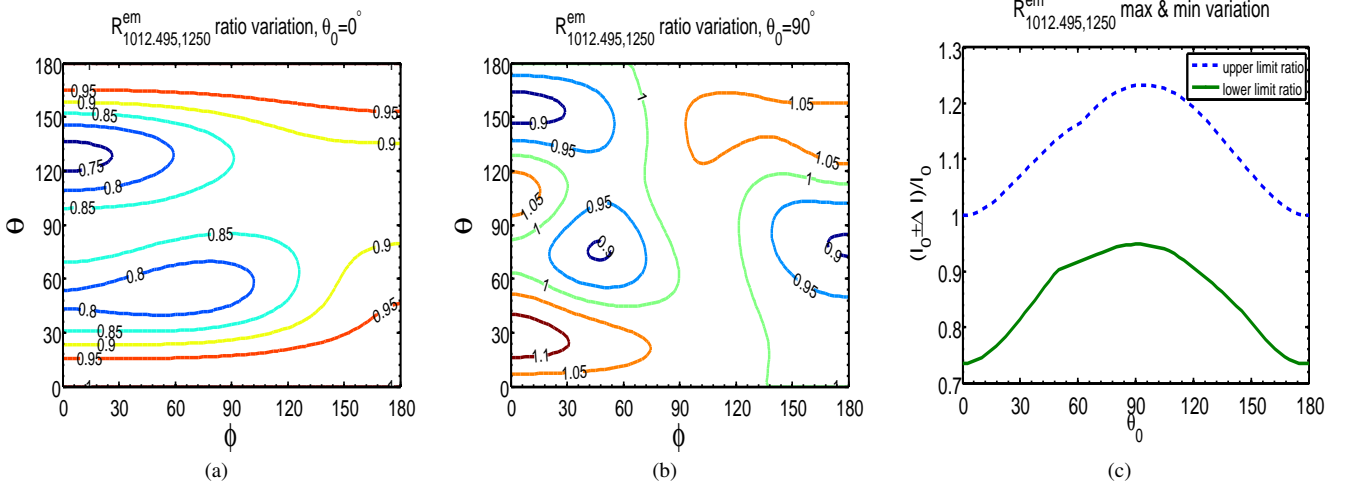


**Figure 9.** Variation of the ionization rate: line ratio of S III  $\lambda$ 1012.49 and S II  $\lambda$ 1250.58 emission line. The line ratio of *case 0* is set as 1. (a),(b) The variation of line ratio with respect to the direction of the magnetic field in the case of line of sight parallel and vertical to radiation field ( $\theta_0 = 0^\circ, 90^\circ$ ), respectively; (c) The maximum and minimum ratio as a function of  $\theta_0$ .

The abundance of the elements is assumed to be equal to the column density of the element in the dominant ionization state. For example, Fe II lines are used for iron abundance and S II for sulfur since in DLAs these elements are mostly single ionized. Thus, the ratio  $N(\text{S})/N(\text{Fe})$  can be obtained by measuring  $\mathcal{R}_{\text{SII,FeII}}^{ab}$ . The variation of the ratio S II/Fe II with respect to different direction of magnetic fields when  $\theta_0 = 90^\circ$  is presented in Fig. 8(a). The maximum and minimum variation for  $N(\text{S})/N(\text{Fe})$  due to GSA, as shown in Fig. 8(b), is  $[-14\%, +10\%]$ , which makes the variation in log-scales  $[-0.07, +0.04]$ .

In comparison, another  $\alpha$  element O is presented as an example. Most oxygen in DLAs are neutral and Therefore the ratio  $N(\text{O})/N(\text{Fe})$  can be represented by  $\mathcal{R}_{\text{OI,FeII}}^{ab}$ . The influence of GSA on the line ratio O I  $\lambda$ 1302.17/Fe II  $\lambda$ 1608.45 when  $\theta_0 = 90^\circ$  is presented in Fig. 8(c). By comparing Fig. 8(a) and Fig. 8(c), it is obvious that when magnetic field is perpendicular to both the line of sight and incidental radiation, the alignment enriches  $N(\text{S})/N(\text{Fe})$  by 10% whereas depletes  $N(\text{O})/N(\text{Fe})$  by 9%. As a result, with the same direction of magnetic field and the same line of sight,  $[\text{S}/\text{Fe}]$  observed varies  $+0.04$  while  $[\text{O}/\text{Fe}]$  observed varies  $-0.06$ . Therefore, GSA will affect on the results from nucleosynthetic studies although the modification is small, in particular when compared to possible ionization effect. The influence is sensitive to the direction of magnetic field.

#### 4.2. Influence on ionization studies in diffuse gas

The line ratio of the different ionization states of the same element is often used to determine the ionization rate (see, e.g., Richter et al. 2016). As an example, (S III)/(S II) emission line ratio is employed to determine the ionization rate in extragalactic H II region (see, e.g., Vilchez et al. 1988), because higher ionized Sulphur is not important in most of these H II regions (Mathis 1982, 1985). To illustrate the influence of GSA, the line ratio S III  $\lambda$ 1012.49/S II  $\lambda$ 1250.58 is adopted to represent (S III)/(S II). Fig. 9(a) and Fig. 9(b) demonstrate the influence of GSA with different direction of magnetic fields when  $\theta_0 = 0^\circ$  and  $90^\circ$ . It is evident that the influence of magnetic field is absolutely different given different  $\theta_0$ . By scanning  $\theta_0$  from  $0^\circ$  to  $180^\circ$  in Fig. 9(c), the range of variation under the influence of GSA is  $[-27\%, +12\%]$ , which means a variation of  $[-0.14, +0.05]$  on  $\log[N(\text{S III})/N(\text{S II})]$ . Obviously, the influence of magnetic field due to GSA on the ionization rate cannot be ignored.

### 5. DISCUSSIONS

Atomic alignment is a well-studied effect in laboratory, whilst its importance still requires attention in astrophysical community. It has been well demonstrated in earlier works that atomic alignment is a universal magnetic tracer in diffuse interstellar medium. The linear polarization induced by atomic alignment changes with respect to the direction of magnetic field. Thus by measuring linear polarization of atomic lines, we can probe the corresponding magnetic direction. Atomic alignment provides us several options to observe: absorption and emission of atomic lines in UV, optical, and submillimeter bands. The effective regime of atomic alignment is very broad (see §2.1). The effect can induce more than 20% of polarization in certain spectral lines (see the review in Yan & Lazarian 2012). It should be a promising physical effect for observation which can provide us independent information to other magnetic diagnostic.

In this paper, we generate synthetic spectra for DLAs in galaxy to demonstrate the modulation of observed spectra from magnetic fields due to GSA. We illustrate the variation of emission lines due to GSA with an example of extragalactic H II Regions. The influence of GSA on submillimeter fine-structure lines is discussed for SFRs. The variations that magnetic field

causes because of GSA effect to the physical parameters derived from spectral line ratios are analysed. Nevertheless, the effect is not limited to the examples that we provide. To achieve a more precise measurement of physical processes, GSA should be taken into account in future studies.

As illustrated in this paper, the modification induced by changing magnetic direction due to GSA varies among different spectral lines. Thus, if multiplet is available in a given line spectrum, the GSA effect will induce differential changes in the line intensity among the multiplet. The effect should be taken seriously for spectra with a high spectral resolution and a high S/N ratio. Furthermore, as illustrated in [Yan & Lazarian \(2007\)](#), hyperfine splitting of atoms and ions will also influence the alignment. Hyperfine splitting has to be considered when studying the GSA effect on fine structure transitions of the atoms with nuclear spin. Even with the same fine structure, the atoms with hyperfine structure is affected by GSA differently than those atoms without nuclear spins<sup>10</sup>. The alignment on different hyperfine sublevels of the same fine structure level can be different. Therefore, they will be perfect for analyzing the influence of magnetic fields because the wavelength span of hyperfine multiplet is so small that they would share the same S/N ratio provided that the intrinsic hyperfine splitting is wider than the thermal/turbulence broadening.

Fluorescence lines are important in studying Gaseous Nebulae. Ultraviolet-pumped infrared fluorescence lines have been applied to the modelling of reflection nebulae ([Sellgren 1984, 1986](#)). Iron fluorescence lines have been used to diagnose the reflection nebulae near the Galactic center ([Muno et al. 2007](#)). They also play an important role in understanding the structure of photodissociation fronts ([Draine & Bertoldi 1996](#)), H II Regions ([Black & van Dishoeck 1987](#)), etc. As illustrated in §3.2, the alignment on the ground state can be transferred to the upper state through absorption process. Therefore, fluorescence lines can also be influenced by magnetic field. The intensity of the lines derived from successive decays to different levels of atoms are thus dependent on the density of the initial upper levels, which can be influenced by GSA by scattering process as demonstrated in [Fig.5](#). The influence of magnetic field on fluorescence lines can be considered in future work.

Most interstellar medium resides in GSA regime ( $1 \text{ Gauss} \gtrsim B \gtrsim 10^{-15} \text{ Gauss}$ , see §2.1 for details), where the influence of magnetic field on spectral lines cannot be neglected. The influence of magnetic fields on photon-excited spectra, though, is not limited to this range. Stronger magnetic fields ( $B > 1 \text{ Gauss}$ ) can also affect the spectra observed (e.g., spectra from photosphere) due to the Hanle effect, which solar physicists have been employing to analyse the strength and direction of the strong magnetic field in the medium close to the local radiative pumping star (see, e.g., [Landi Degl’Innocenti & Landolfi 2004](#)). For much weaker magnetic field or stronger radiation source so that that the radiative pumping on ground level is comparable to the magnetic precession rate ( $\nu_L \sim B_{lu} J_0^0$ ), spectral lines can be also modulated by the lower level Hanle effect.

The influence of collision is neglected in this paper, which applies to most diffuse interstellar medium. However, collision can become important in the case of higher density and higher temperature medium. Collisions reduce the alignment efficiency (see [Hawkins 1955](#)). When the collision rate  $\tau_c^{-1}$  (either inelastic collision rate or Van der Waals collision rate) dominates over optical pumping rate  $B_{J_l J_u} I$  (see [Yan & Lazarian 2006](#) for details), alignment is destroyed. The effect of collisions will be evaluated in future work.

## 6. SUMMARY

We have demonstrated the influence of magnetic fields due to GSA effect on spectroscopic studies. We emphasize that GSA is a generic physical process that can induce systematic variation to both absorption and emission spectral lines observed from diffuse interstellar medium. The astrophysical environments that are in GSA regime include DLAs, H II Regions, PDRs, SFRs, Herbig Ae/Be disks, etc. Examples of absorption, emission and submillimeter fine-structure lines observed from different astrophysical environments have been presented in the paper to illustrate the influence of magnetic field due to GSA. Variations of line ratios are presented. The influence of magnetic field on spectral line ratio is more significant and can reach more than 25% in some cases. Our main conclusions are:

- Due to GSA, magnetic fields will affect absorption and emission spectral lines from diffuse interstellar medium.
- Physical parameters derived from line ratios can be influenced by magnetic field.
- The depletion and enrichment of the same spectrum change in accordance with the direction of magnetic field.
- The modification of the line intensity with respect to the magnetic field varies among different spectral lines.

<sup>10</sup> See the comparison between the alignment of S II and N I in [Yan & Lazarian 2007](#), in which the two elements share the same atomic fine structure, but due to a different nuclear spin, the alignment on the ground state of the two elements are totally different.

## APPENDIX

## A. BASIC FORMULAE ON ATOMIC ALIGNMENT

In this Appendix, we illustrate the basic equations on GSA and address the point in §2 on how the magnetic fields affect the density of atoms on ground level  $\rho(J_l)$  due to GSA. The calculations in this Appendix are all performed in the theoretical frame  $x'y'z'$ -system in Fig.1(b).

Anisotropic radiation can excite atoms, which is known as photo-excitation and consequently results in spontaneous emissions. Occupations of the atoms on different sublevels of the ground state will alter when there exists anisotropic radiation field. With the existence of magnetic fields, the angular momenta of the atoms will redistribute among the sublevels on the ground state due to fast magnetic precession, which is termed as magnetic realignment (see [Yan & Lazarian 2012, 2015](#) for details). The equations to describe the evolution of atom densities on both upper and ground states are (see [Landolfi & Landi Degl'Innocenti 1986](#); [Landi Degl'Innocenti & Landolfi 2004](#)):

$$\begin{aligned} \dot{\rho}_q^k(J_u) + 2\pi i \nu_L g_u q \rho_q^k(J_u) = \\ - \sum_{J_l} A(J_u \rightarrow J_l) \rho_q^k(J_u) + \sum_{J_l k'} [J_l] \left[ \delta_{kk'} p_{k'}(J_u, J_l) B_{lu} \bar{J}_0^0 + \sum_{Qq'} r_{kk'}(J_u, J_l, Q, q') B_{lu} \bar{J}_Q^2 \right] \rho_{-q'}^{k'}(J_l), \end{aligned} \quad (\text{A1})$$

$$\begin{aligned} \dot{\rho}_q^k(J_l) + 2\pi i \nu_L g_l q \rho_q^k(J_l) = \\ \sum_{J_u} p_k(J_u, J_l) [J_u] A(J_u \rightarrow J_l) \rho_q^k(J_u) - \sum_{J_u k'} \left[ \delta_{kk'} B_{lu} \bar{J}_0^0 + \sum_{Qq'} s_{kk'}(J_u, J_l, Q, q') B_{lu} \bar{J}_Q^2 \right] \rho_{-q'}^{k'}(J_l), \end{aligned} \quad (\text{A2})$$

in which

$$p_k(J_u, J_l) = (-1)^{J_u + J_l + 1} \begin{Bmatrix} J_l & J_l & k \\ J_u & J_u & 1 \end{Bmatrix}, \quad p_0(J_u, J_l) = \frac{1}{\sqrt{[J_u, J_l]}}, \quad (\text{A3})$$

$$r_{kk'}(J_u, J_l, Q, q) = (3[k, k', 2])^{\frac{1}{2}} \begin{Bmatrix} 1 & J_u & J_l \\ 1 & J_u & J_l \\ 2 & k & k' \end{Bmatrix} \begin{pmatrix} k & k' & K \\ q & q' & Q \end{pmatrix}, \quad (\text{A4})$$

$$s_{kk'}(J_u, J_l, Q, q) = (-1)^{J_l - J_u + 1} [J_l] (3[k, k', K])^{\frac{1}{2}} \begin{pmatrix} k & k' & 2 \\ q & q' & Q \end{pmatrix} \begin{Bmatrix} 1 & 1 & 2 \\ J_l & J_l & J_u \end{Bmatrix} \begin{Bmatrix} k & k' & 2 \\ J_l & J_l & J_l \end{Bmatrix}. \quad (\text{A5})$$

The evolution of the ground state  $[\rho_q^k(J_l)]$  and the upper state  $[\rho_q^k(J_u)]$  are illustrated in Eq. (A2) and Eq. (A1), respectively. The quantities  $J_u$  and  $J_l$  are the total angular momentum quantum numbers for the upper and lower levels, respectively. The quantity  $A$  and  $B$  are Einstein coefficients for emission and absorption. The quantities  $\rho_q^k$  and  $\bar{J}_Q^K$  are irreducible density matrices for the atoms and the radiation field, respectively.  $6-j$  and  $9-j$  symbols are represented by the matrices with “{ }”, whereas  $3-j$  symbols are indicated by the matrices with “( )” (see [Zare & Harter 1989](#) for details). The symbol  $[j]$  represents the quantity  $2j+1$ , e.g.,  $[J_l] = 2J_l + 1$ ,  $[J_l, J_u] = (2J_l + 1)(2J_u + 1)$ , etc. *The second terms on the left side of Eq. (A1) and Eq. (A2) stand for the magnetic realignment.* The two terms on the right side represent spontaneous emissions and the excitations from lower levels. All the transitions to different upper states and different sublevels of the ground state are taken into account by summing up  $J_u$  and  $J_l$ . Note that the symmetric processes of spontaneous emission and magnetic realignment conserve  $k$  and  $q$ . Therefore, the steady state occupations of atoms on the ground state are obtained by setting the left side of Eq. (A1) and Eq. (A2) zero<sup>11</sup>:

$$\begin{aligned} 2\pi i \rho_q^k(J_l) q g_l \nu_L - \sum_{J_u k'} \left\{ p_k(J_u, J_l) \frac{[J_u]}{\sum_{J_l''} A''/A + i\Gamma' q} \sum_{J_l'} B_{lu} [J_l'] \left[ \delta_{kk'} p_{k'}(J_u, J_l') \bar{J}_0^0 + \sum_{Qq'} r_{kk'}(J_u, J_l', Q, q') \bar{J}_Q^2 \right] \right. \\ \left. - \delta_{J_l J_l'} \left[ \delta_{kk'} B_{lu} \bar{J}_0^0 + \sum_{Qq'} B_{lu} s_{kk'}(J_u, J_l, Q, q') \bar{J}_Q^2 \right] \right\} \rho_{-q'}^{k'}(J_l) = 0 \end{aligned} \quad (\text{A6})$$

<sup>11</sup> This is the correct version of Eq. (8) in [Yan & Lazarian \(2008\)](#), in which there is a typo. The term  $\Gamma$  in Eq. (8) of [Yan & Lazarian \(2008\)](#) denotes  $B_{lu}$  as a common factor. But that will be an error for multi-level atoms because the Einstein coefficients for transitions between different upper and lower levels are different.

where  $\Gamma'$  equals  $2\pi\nu_L g_u/A$ . As illustrated in §2.1, magnetic realignment on the upper levels can be neglected due to fast magnetic precession ( $A \gg \nu_L$ ) as long as the strength of magnetic field is below the GSA upper regime. As a result,  $\Gamma' \sim 0$ . On the other hand, GSA lower regime requires  $\nu_L \gg B_{lu} J_0^0$ . Thus, Eq. (A6) is making sense only when  $q = 0$  so that the first term on the left equals 0. Solving the above equations, the density of atoms on different levels,  $\rho_q^k(J_l)$  and  $\rho_q^{k'}(J_u)$ , under the influence of magnetic fields can be obtained.

## REFERENCES

- Armstrong, J. W., Rickett, B. J., & Spangler, S. R. 1995, *ApJ*, 443, 209  
 Asplund, M., Grevesse, N., Sauval, A. J., & Scott, P. 2009, *ARA&A*, 47, 481  
 Black, J. H., & van Dishoeck, E. F. 1987, *ApJ*, 322, 412  
 Bommier, V., & Sahal-Brechot, S. 1978, *A&A*, 69, 57  
 Brown, J. C., & Taylor, A. R. 2001, *ApJL*, 563, L31  
 Chepurnov, A., Gordon, J., Lazarian, A., & Stanimirovic, S. 2008, *ApJ*, 688, 1021  
 Coil, A. L., Aird, J., Reddy, N., et al. 2015, *ApJ*, 801, 35  
 Cooke, R., Pettini, M., Steidel, C. C., Rudie, G. C., & Nissen, P. E. 2011, *MNRAS*, 417, 1534  
 Crutcher, R., Heiles, C., & Troland, T. 2003, in *Lecture Notes in Physics*, Berlin Springer Verlag, Vol. 614, *Turbulence and Magnetic Fields in Astrophysics*, ed. E. Falgarone & T. Passot, 155–181  
 Dehmelt, H. G. 1957, *Physical Review*, 105, 1487  
 Díaz-Santos, T., Armus, L., Charmandaris, V., et al. 2013, *ApJ*, 774, 68  
 Dinerstein, H. L., Sterling, N. C., & Bowers, C. W. 2006, in *Astronomical Society of the Pacific Conference Series*, Vol. 348, *Astrophysics in the Far Ultraviolet: Five Years of Discovery with FUSE*, ed. G. Sonneborn, H. W. Moos, & B.-G. Andersson, 328  
 D’Onghia, E., & Fox, A. J. 2016, *ARA&A*, 54, 363  
 Draine, B. T. 1978, *ApJS*, 36, 595  
 Draine, B. T., & Bertoldi, F. 1996, *ApJ*, 468, 269  
 D’Yakovon, M. I., & Perel’, V. I. 1965, *Soviet Journal of Experimental and Theoretical Physics*, 21, 227  
 Esteban, C., García-Rojas, J., Carigi, L., et al. 2014, *MNRAS*, 443, 624  
 Fano, U. 1957, *Reviews of Modern Physics*, 29, 74  
 Fontana, A., & Ballester, P. 1995, *The Messenger*, 80, 37  
 Fox, A., Richter, P., & Fechner, C. 2014a, *A&A*, 572, A102  
 Fox, A. J., Richter, P., Wakker, B. P., et al. 2013, *ApJ*, 772, 110  
 Fox, A. J., Wakker, B. P., Barger, K. A., et al. 2014b, *ApJ*, 787, 147  
 Fynbo, J. P. U., Starling, R. L. C., Ledoux, C., et al. 2006, *A&A*, 451, L47  
 García-Rojas, J., Corradi, R. L. M., Monteiro, H., et al. 2016, *ApJL*, 824, L27  
 Hawkins, W. B. 1955, *Physical Review*, 98, 478  
 Hawkins, W. B., & Dicke, R. H. 1953, *Phys. Rev.*, 91, 1008  
 Hogerheijde, M. R., Jansen, D. J., & van Dishoeck, E. F. 1995, *A&A*, 294, 792  
 House, L. L. 1974, *PASP*, 86, 490  
 Kama, M., Bruderer, S., Carney, M., et al. 2016, *A&A*, 588, A108  
 Kastler, A. 1950, *J. Phys. Radium*, 11, 255  
 Kaufman, M. J., Wolfire, M. G., Hollenbach, D. J., & Luhman, M. L. 1999, *ApJ*, 527, 795  
 Kisielius, R., Kulkarni, V. P., Ferland, G. J., Bogdanovich, P., & Lykins, M. L. 2014, *ApJ*, 780, 76  
 Kobulnicky, H. A., Kennicutt, Jr., R. C., & Pizagno, J. L. 1999, *ApJ*, 514, 544  
 Landi Degl’Innocenti, E. 1983, *SoPh*, 85, 3  
 —. 1984, *SoPh*, 91, 1  
 —. 1998, *Nature*, 392, 256  
 Landi Degl’Innocenti, E., & Landolfi, M., eds. 2004, *Astrophysics and Space Science Library*, Vol. 307, *Polarization in Spectral Lines*  
 Landolfi, M., & Landi Degl’Innocenti, E. 1986, *A&A*, 167, 200  
 Lehner, N., Wakker, B. P., & Savage, B. D. 2004, *ApJ*, 615, 767  
 Leitherer, C., Hernandez, S., Lee, J. C., & Oey, M. S. 2016, *ApJ*, 823, 64  
 Maaskant, K. M., Honda, M., Waters, L. B. F. M., et al. 2013, *A&A*, 555, A64  
 Mathis, J. S. 1982, *ApJ*, 261, 195  
 —. 1985, *ApJ*, 291, 247  
 McWilliam, A. 1997, *ARA&A*, 35, 503  
 Meiring, J. D., Tripp, T. M., Prochaska, J. X., et al. 2011, *ApJ*, 732, 35  
 Morton, D. C. 2003, *ApJS*, 149, 205  
 Muno, M. P., Baganoff, F. K., Brandt, W. N., Park, S., & Morris, M. R. 2007, *ApJL*, 656, L69  
 Peimbert, M., & Peimbert, A. 2006, in *IAU Symposium*, Vol. 234, *Planetary Nebulae in our Galaxy and Beyond*, ed. M. J. Barlow & R. H. Méndez, 227–234  
 Prochaska, J. X., & Wolfe, A. M. 2002, *ApJ*, 566, 68  
 Prochaska, J. X., Wolfe, A. M., Tytler, D., et al. 2001, *ApJS*, 137, 21  
 Rao, S. M., & Turnshek, D. A. 2000, *ApJS*, 130, 1  
 Richter, P., Fox, A. J., Wakker, B. P., et al. 2013, *ApJ*, 772, 111  
 Richter, P., Sembach, K. R., Wakker, B. P., et al. 2001, *ApJ*, 559, 318  
 Richter, P., Wakker, B. P., Fechner, C., et al. 2016, *A&A*, 590, A68  
 Salgado, F., Berné, O., Adams, J. D., et al. 2016, *ApJ*, 830, 118  
 Savage, B. D., & Sembach, K. R. 1996, *ARA&A*, 34, 279  
 Sellgren, K. 1984, *ApJ*, 277, 623  
 —. 1986, *ApJ*, 305, 399  
 Shanguan, J., & Yan, H. 2013, *Ap&SS*, 343, 335  
 Stenflo, J. O., & Keller, C. U. 1997, *A&A*, 321, 927  
 Trujillo Bueno, J., & Landi Degl’Innocenti, E. 1997, *ApJL*, 482, L183  
 Van Vleck, J. H. 1925, *Proceedings of the National Academy of Science*, 11, 612  
 Varshalovich, D. A. 1968, *Astrofizika*, 4, 519  
 —. 1971, *Soviet Physics Uspekhi*, 13, 429  
 Vilchez, J. M., Pagel, B. E. J., Diaz, A. I., Terlevich, E., & Edmunds, M. G. 1988, *MNRAS*, 235, 633  
 Welsh, B. Y., & Lallement, R. 2012, *PASP*, 124, 566  
 Wills, B. J., Netzer, H., & Wills, D. 1985, *ApJ*, 288, 94  
 Yan, H., & Lazarian, A. 2006, *ApJ*, 653, 1292  
 —. 2007, *ApJ*, 657, 618  
 —. 2008, *ApJ*, 677, 1401  
 —. 2012, *JQSRT*, 113, 1409  
 Yan, H., & Lazarian, A. 2015, in *Astrophysics and Space Science Library*, Vol. 407, *Magnetic Fields in Diffuse Media*, ed. A. Lazarian, E. M. de Gouveia Dal Pino, & C. Melioli, 89  
 Youngblood, A., Ginsburg, A., & Bally, J. 2016, *AJ*, 151, 173  
 Zare, R. N., & Harter, W. G. 1989, *Physics Today*, 42, 68  
 Zech, W. F., Lehner, N., Howk, J. C., Van Dyke Dixon, W., & Brown, T. M. 2008, *ApJ*, 679, 460  
 Zhang, H., Yan, H., & Dong, L. 2015, *ApJ*, 804, 142